Arch. Metall. Mater. **66** (2021), 1, 229-239

DOI: 10.24425/amm.2021.134780

Q. AN[1], K.Y. FAN[1], Y.F. GE[1], B.X. LIU[1*], J. HE[1*], S. WANG[1], C.X. CHEN[1], P.G. JI[1,2], O. TOLOCHKO[2]

THE BENDING, IMPACT FRACTURE BEHAVIOR AND CHARACTERISTICS OF STAINLESS STEEL CLAD PLATES WITH DIFFERENT ROLLING TEMPERATURE

The interface characteristics, bending and impact behavior, as well as fracture characteristics of stainless steel clad plates fabricated by vacuum hot rolling at different rolling temperatures of 1100°C, 1200°C and 1300°C are investigated in detail. The interface bonding strength is gradually increased with the increasing rolling temperature due to the sufficient diffusion behavior of alloy element. The bending toughness and impact toughness are gradually decreased, while the bending strength increase with the increase of the rolling temperature, which is attributed to mechanisms of matrix softening and interface strengthening at high rolling temperature. Due to the weak interface at 1100°C, the bending and impact crack propagation path was displaced by delamination cracks, which in turn lead to reduction in stress intensity of the main crack, playing an effective role in toughening the stainless steel clad plates. Moreover, the impact fracture morphologies of clad plates show a typical ductile-brittle transition phenomenon, which is attributed to the matrix softening behavior with the increasing rolling temperature.

Keywords: stainless steel clad plate, interface characteristics, bending behavior, impact morphologies, delamination crack

1. Introduction

Stainless steel clad plates set structure, display function at an organic whole by combining the good high temperature mechanical properties, corrosion resistance, wear resistance, non-magnetic and decorative of clad metal and outstanding weld ability, room temperature mechanical properties and low cost of the base metal [1-3], which have been attracted more and more attentions in high-end defense field, such as nuclear, shipbuilding, petrochemical, armor and desalination sector etc. [4,5], and ninety percents of stainless steel clad plates were produced by vacuum hot rolling method [6]. Herein, some alloying elements such as Fe, Ni, and Cr all diffuse along the clad interface [7-9]. The diffusion behavior of alloying elements play important roles in strengthening and toughening clad interface, and rolling temperature may significantly affect the diffuse velocity and diffuse distance of alloying elements. Therefore, clad interfacial bonding strength is related to the rolling temperature [10,11].

Interface characteristics and bonding strength can result in the different mechanical behavior and properties. In the previous work, the strong interfacial bonding strength delayed the premature localized necking of base metal, which is beneficial to improving uniform plastic deformation capacity of overall clad plate [11,12]. However, weak interfacial bonding strength is good for the bending, fatigue and impact testing [13-16]. In the multilayer composites or clad plate, the toughness can be enhanced by interfacial delamination crack, absorbing a lot of fracture energy [12,17]. Yin et al. [18] obtained the laminated fibrous structure of steel by warm groove rolling, and the interface of elongated fibrous grains is easy to induce delamination crack during the low-temperature impact testing, which is similar to the bending fracture phenomenon of chopsticks and bamboo, revealing an obvious inverse temperature effect of impact property [19]. Therefore, the low-temperature impact toughness can be enhanced by reasonable interfacial bonding strength. Lee et al. [20] reported that laminated super high carbon steel (UHCS)/brass composite obtains superior impact toughness, and ductile brass layers can effectively inhibit the crack propagation, so that UHCS layers are free of notches, and ductile behavior is observed down to liquid nitrogen temperature. Liu et al. [15] investigated the bending fracture characteristics of laminated Ti-TiBw/Ti composites, and proposed that superior fracture

[1] HEBEI UNIVERSITY OF TECHNOLOGY, RESEARCH INSTITUTE FOR ENERGY EQUIPMENT MATERIALS SCHOOL OF MATERIALS SCIENCE AND ENGINEERING, TIANJIN KEY LABORATORY OF MATERIALS LAMINATING FABRICATION AND INTERFACIAL CONTROLLING TECHNOLOGY, TIANJIN 300130, CHINA
[2] PETER THE GREAT SAINT-PETERSBURG POLYTECHNIC UNIVERSITY, MATERIALS SCIENCE DEPARTMENT, SAINT-PETERSBURG, 195251, RUSSIA

* Corresponding author: liubaoxiliubo@126.com)

toughness can be related to the interfacial delamination and tunnel crack synergy toughening mechanisms. Song et al. [21] revealed that natural shells have interfacial delamination and mineral bridge structure, benefiting 2000 times fracture toughness than the conventional $CaCO_3$.

Stainless steel clad plates are comprised of clad interface and carbon diffusion zone, which are the weakest positions affecting the subsequent deformation and forming behavior, however, these topics have yet to be investigated systematically. The previous work has built the relationship between the tensile, shear properties of stainless steel clad plates and rolling temperature in detail [10,11]. However, the carbon diffusion zone and interfacial bonding strength can be severely influenced by rolling temperature. Therefore, investigating the effect of rolling temperature on bending and impact behavior can make a guild to improve the loading capacity and service applications.

2. Experimental procedures

The raw base metal and clad metal of three groups of stainless steel clad plates used in this work were Q235 carbon steel and SUS304 stainless steel, respectively, and the chemical compositions of those commercial hot rolling plates are listed in Table 1.

TABLE 1

The chemical composition of the carbon steel and stainless steel (wt. %)

Elements	Fe	Cr	Ni	C	Mn	Si	P	S
Q235	98.91	—	—	0.2	0.5	0.3	0.045	0.05
SUS304	68.95	18.5	8.5	0.025	2	2	0.025	0.001

Carbon steel plates with dimension of 200×240×60 mm and SUS304 stainless steel plates with dimension of 160×200×12 mm were prepared for hot-rolling preparation. Two groups of square billets were mirror symmetrically assembled after cleaning up the oxide scale and containment layer on the surface by angle grinder or other grinding machines. All round weld of plates edges was carried out to form a sealed chamber with a reserved air exhaust hole, then vacuuming was performed with 10^{-2} Pa and sealing state for holding through the hot rolling process. The rolling process was carried out after soaking the built-up slab at 1100°C, 1200°C and 1300°C for 120 min. The thicknesses of the clad plates were reduced from 145 mm to 14 mm after eight passes in about 5 min, and total rolling reduction ratio is 90.3%. Finally, the hot products were naturally cooled in air and afterwards cut for testing.

Cross sections parallel to the rolling direction of the clad plates with 10mm interface were ground and finished to detect the interface microstructure and characteristics by optical microscopy (OM) and scanning electrical microscopy (SEM). The samples were sequentially etched with 4% ethanol solution of nitric acid and 10% chromic acid electrolytic method for microstructure observation. Interface alloying elements diffusion behavior was investigated using electron probe microanalysis (EPMA) with wavelength dispersive spectroscopy (WDS). Bending specimens with notch crack and impact samples were machined parallel to the rolling direction with modes I, II and III as shown in Fig. 1. The bending and impact fracture characteristics were also conducted using a scanning electron microscope (SEM) and digital camera. A total of five samples were tested for each mode. The bending load-displacement (F-l) curve was acquired automatically by using an instron-5500 electronic universal test machine at room temperature.

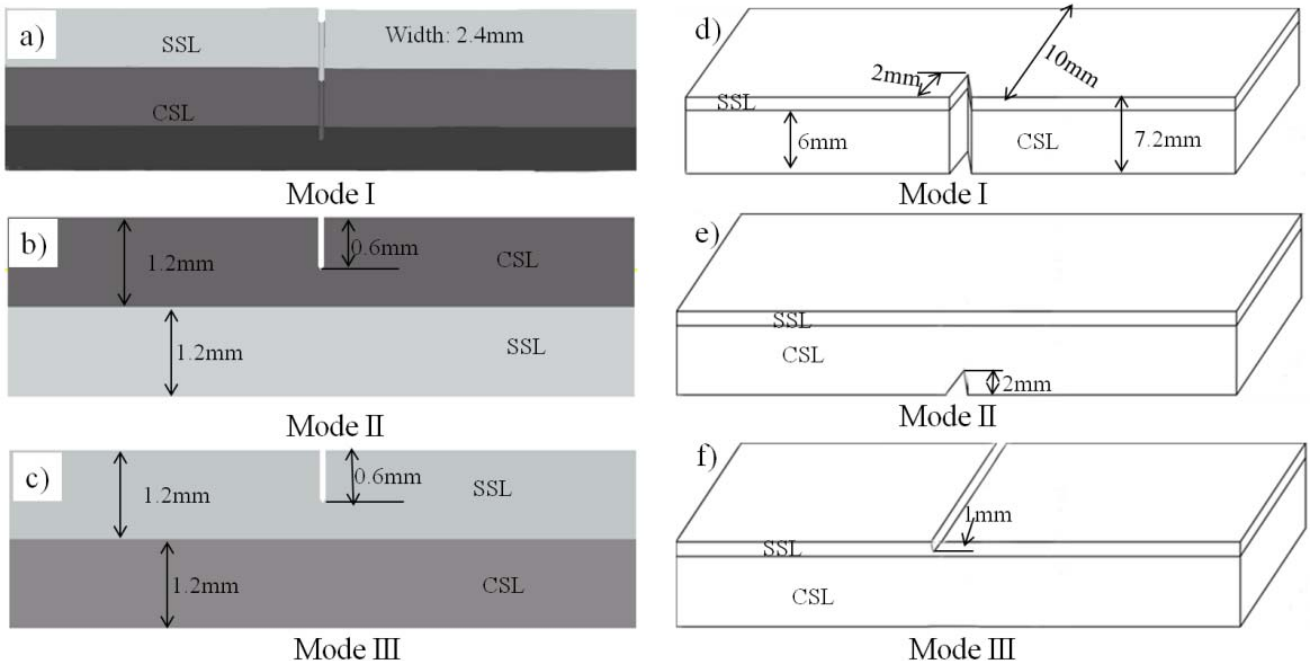

Fig. 1. The schematic diagrams of notched bending samples under a)mode I; b) mode II; c) mode III and notched impact samples under d) mode I; e) mode II; f) mode III

3. Results and discussions

3.1. Microstructure and interface alloying element distribution

Fig. 2 shows the interface microstructure and characteristics of stainless steel clad plates fabricated at different rolling temperature. During the hot rolling process, carbon element from base metal diffuse into the clad metal and result in the formation of decarburized layer full of ferrite phases. Meanwhile, a carburized layer of clad metal formed due to the diffusion behavior of carbon element [22-25]. The grain boundaries of carburized layer are ornamented by many chromium carbide ($Cr_{23}C_6$), which leads to low corrosion resistance and intergranular corrosion crack tendency. The carbon element diffusion zone and grain size gradually increase with the increasing rolling temperature. Stainless steel clad plates fabricated at 1100°C, 1200°C and 1300°C obtained decarburized layers with thicknesses of 75 μm, 91 μm and 96 μm, respectively. Compared with the little change of decarburized layer, the thicknesses of carburized layer are 33 μm, 108 μm and 160 μm, respectively, which changed a lot. That is to say, the carbon diffusion behavior in the austenite phase rather than the ferrite phase can be severely affected by rolling temperature, and the carbon diffusion behavior becomes obvious at high temperature.

Fig. 3 shows the diffusion behavior of interface alloying elements, such as Fe, Ni, Cr, C elements. Obviously, the diffusion distance of all the alloying elements gradually extend with the increase of rolling temperature. The diffusion distance of Fe, Cr, Ni elements at 1100°C are 3 μm, 5 μm and 2 μm, respectively. The clad plate fabricated at 1200°C obtains a thick diffusion zone with the diffusion distance of Fe, Cr, Ni elements are 8 μm, 10 μm and 7 μm, respectively. However, when the rolling temperature reaches to 1300°C, the Fe, Cr, Ni elements diffuse about 15 μm, 20 μm and 8 μm, respectively. In the previous work, Chen et al. [10] reported that stainless steel clad plates with strong interface bonding strength are mainly attributed to the sufficient diffusion of interface alloying elements and recovery, recrystallization of interface microstructure. Interface formation process is related to the nucleation, growth of sinter necking, converge of interface pores and formation of grain boundary [12,26-28]. Meanwhile, alloy element diffusion plays an important role in strengthening and toughening interface by solid solution strengthening and dispersion strengthening mechanisms. The thicker of the alloy diffusion distance, the stronger of the interfacial bonding strength of clad plates. Moreover, the carbon element reveals a peak value and uphill diffusion phenomena at the interface zone detected by EPMA, and the carbon content of carburized layer is higher than that of decarburized layer, which is fitting to the results of Pavlovsky et al. [29]. It is attributed to the different diffusion velocity and solubility of carbon element in ferrite and austenite, respectively, and the ferrite has high diffusion velocity and low solubility of carbon element compared to the austenite [30,31].

Fig. 4 shows the bending load-displacement curves of stainless steel clad plates fabricated at different rolling temperatures under modes I, II and III. No matter what mode of notched crack is, the deformation characteristics are basically same. With the increase of rolling temperature, the maximum bending loading force gradually decrease as shown in Figs. 3a)-c), which may be attributed to the matrix softening and grain coarsening mechanisms. However, the bending ductility is increase first and then decrease and less pop-in points are presented in the load-displacement curves at high rolling temperature, which may be attributed to the interface bonding status. Stainless steel clad plate fabricated at 1200°C reveals a reasonable interface bonding strength. It can result in the interface delamination crack and long crack propagation path. Meanwhile, the short delamination crack

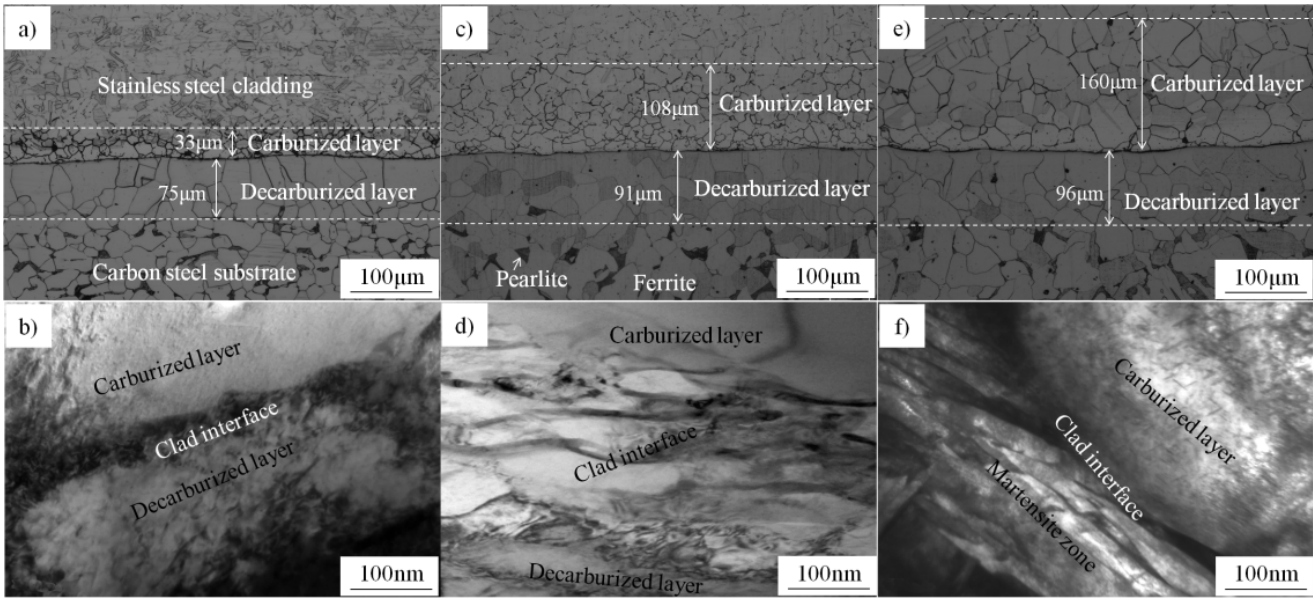

Fig. 2. The microstructure and interface characteristics of stainless steel clad plates fabricated at different rolling temperature. a) 1100°C; b) 1200°C; c) 1300°C

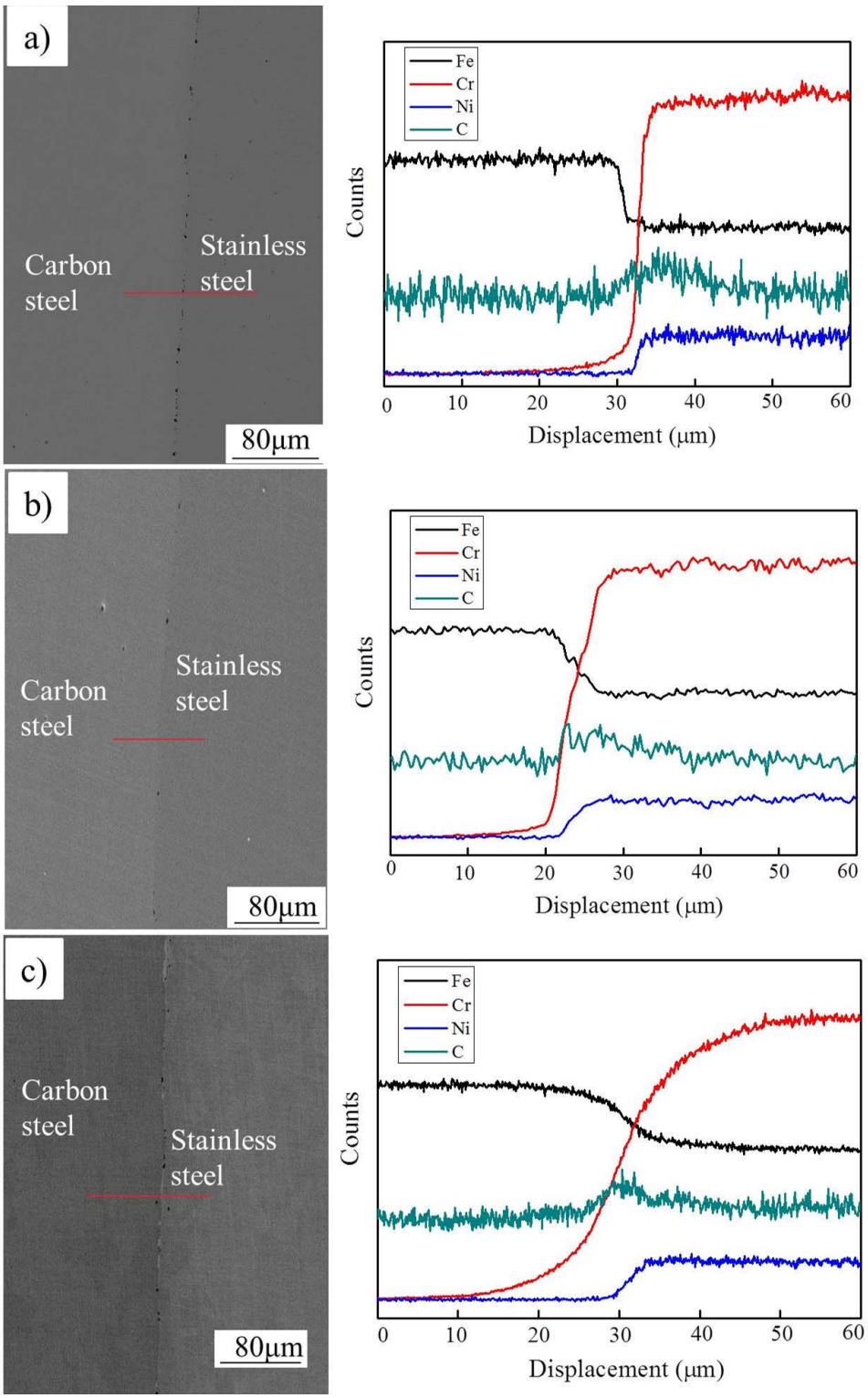

Fig. 3. EPMA analysis shows interface alloying elements diffusion behavior of stainless steel clad plates fabricated at different rolling temperature. a) 1100°C; b) 1200°C; c) 1300°C

plays an important role in synergy strengthening and toughening interface in comparison with long delamination crack, leading to the highest bending toughness [21].

The normal bending fracture morphologies of stainless steel clad plate under divider direction (mode I) are shown in Fig. 5. At the rolling temperature of 1100°C, an obvious long delamination crack with the length of 800~1200 μm present at the clad interface as shown in Figs. 5a)-c), revealing the weak interface bonding strength. At the rolling temperature of 1200°C, the interface delamination crack with the length of 100 μm corresponding with moderate interface bonding strength is shown in Figs. 5d)-f). However, when the rolling temperature reaches to 1300°C, a strong clad interface without interface delamination is shown in Figs. 5g)-i).

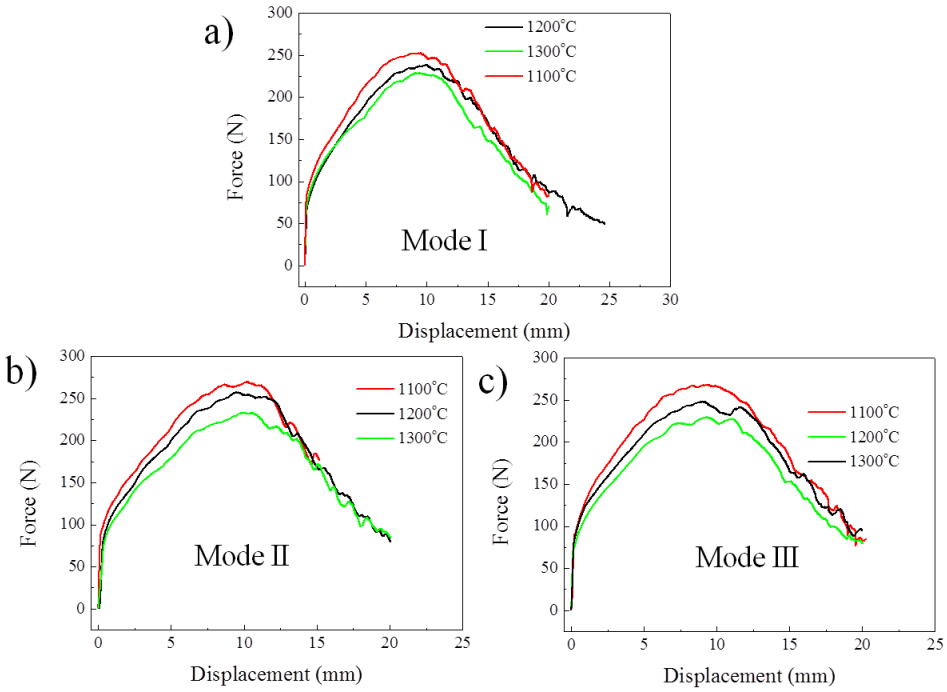

Fig. 4. The bending load-displacement curves of stainless steel clad plates fabricated at different rolling temperatures under modes I (a), II (b) and III (c)

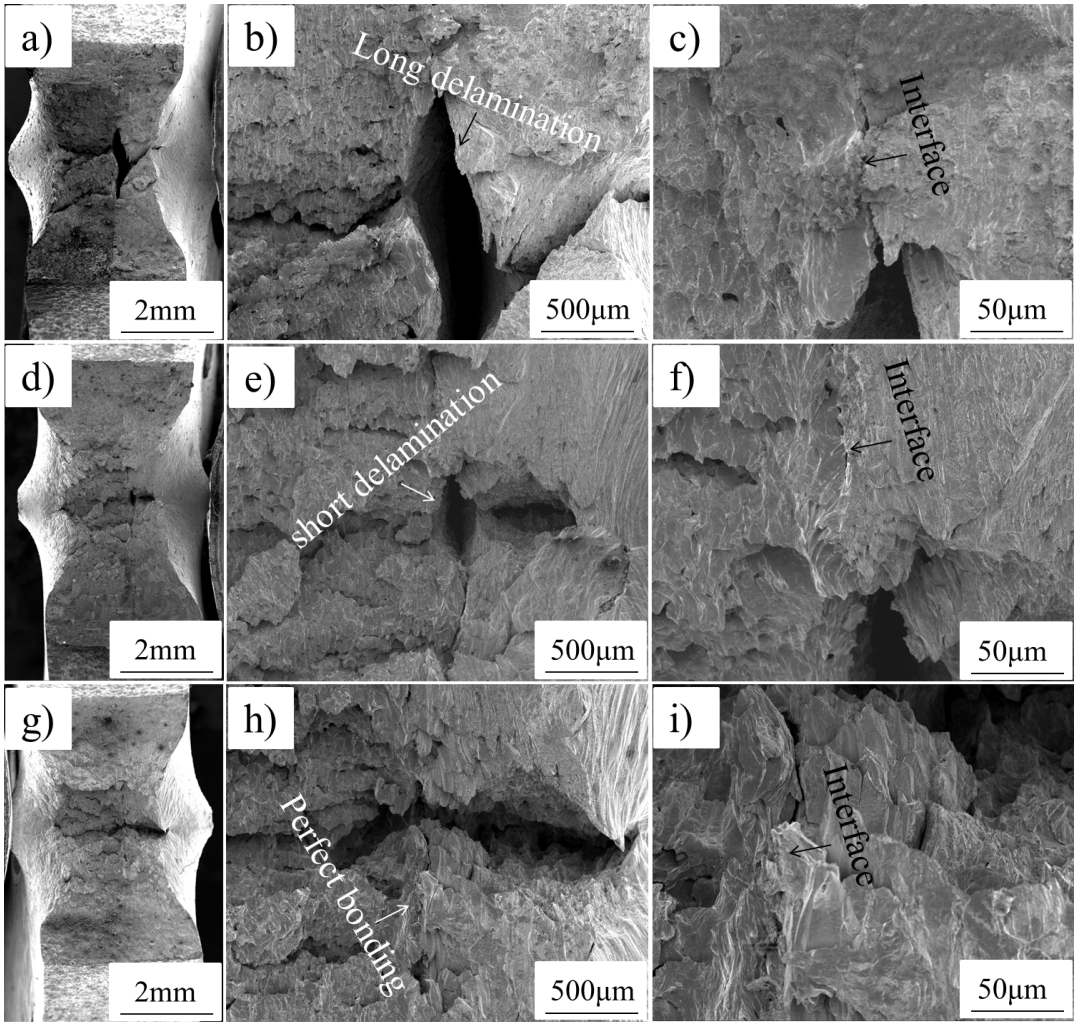

Fig. 5. The normal bending fracture morphologies of stainless steel clad plates fabricated at different temperatrues of a)-c) 1100°C; d)-f) 1200°C; g)-i) 1300°C under mode I

Fig. 6 shows the profile bending fracture morphologies of stainless steel clad plates under arrester direction (modes II and III). Whatever mode II or III, the main crack propagation always induces the formation of obvious interface delamination crack when the rolling temperature reaches to 1100°C as shown in Figs. 6a) and 6b), and the length of delamination crack is about 2 mm. According to the theory of fracture mechanics, the long interfacial delamination crack has great influence on the fracture failure, and severely lowered the fracture toughness of laminated composites [21,32,33]. Li et al. [16,34,35] reported that two typical stresses act around the main crack tip. Stress parallel to the external force shows a maximum value at the crack tip, whereas stress with the direction perpendicular to the external force has a maximum value located somewhere ahead of the main crack tip. Therefore, if there is a weak interface ahead of the main crack, the interface can be opened up before the main crack reaches it. When the rolling temperature reaches to 1200°C, a reasonable short interfacial delamination crack with the length of 300 μm present due to the moderate interface bonding strength as shown in Figs. 6c) and 6d). The short interface delamination crack induces the crack deflection mechanism by consuming a great amount of fracture energy. Therefore, the clad plate fabricated at 1200°C obtains the modest fracture resistance. When the rolling temperature reaches to 1300°C, there are no obvious interface delamination crack during the bending process as shown in Figs. 6e) and 6f), revealing superior interface bonding strength of stainless steel clad plates fabricated at 1300°C compared to 1100°C and 1200°C. Under mode II, the main crack at the base metal is arrested at the interface zone by the blunting of interface and clad metal, accompanying with many crack branches presented at the interface as shown in Fig. 6e). It is because that the carbon steel around clad interface affords super-high tensile

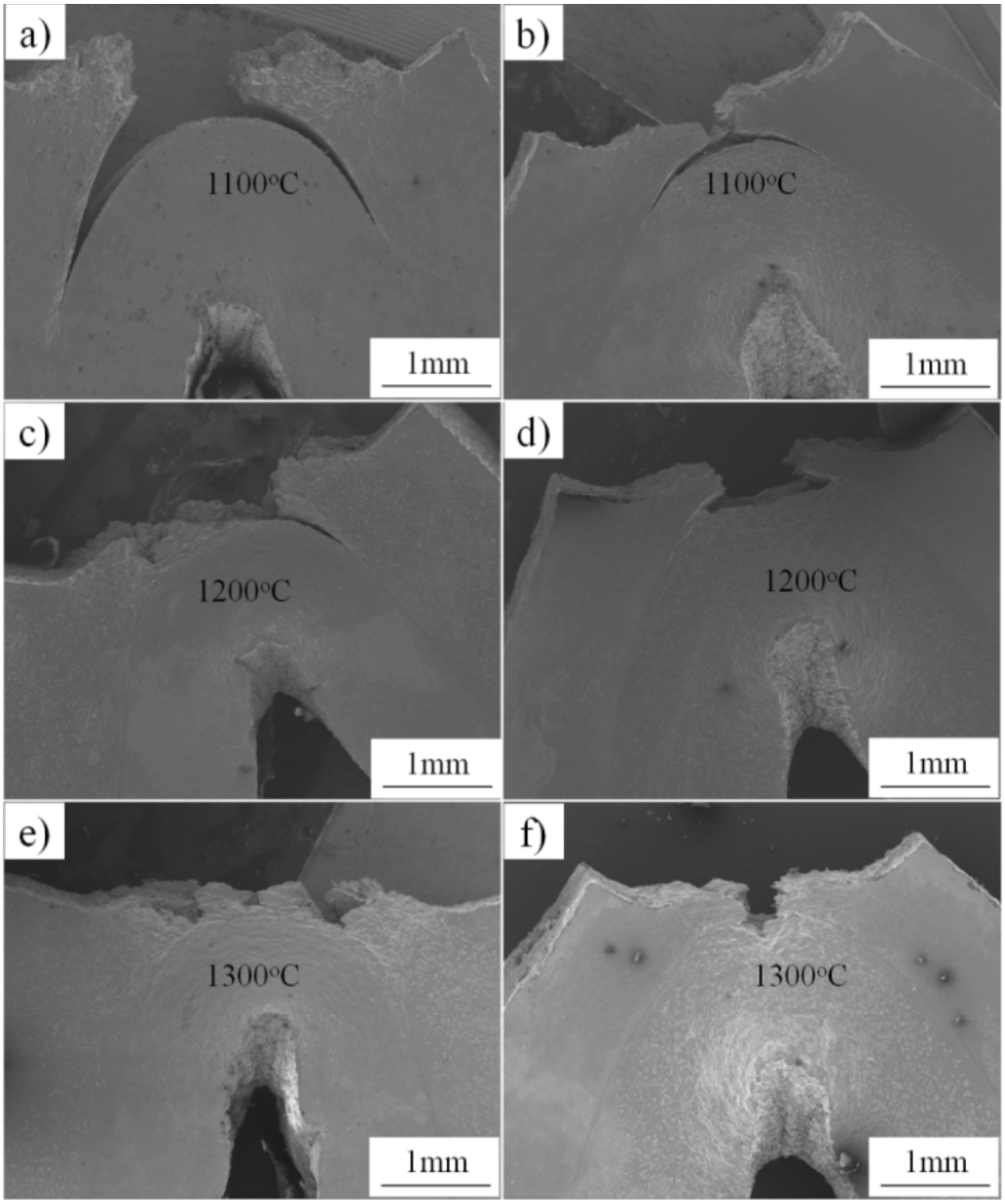

Fig. 6. The profile bending fracture characteristics of stainless steel clad plates fabricated at different temperature of a) 1100°C, mode II; b)1100°C, mode III; c) 1200°C, mode II; d)1200°C, mode III; e) 1300°C, mode II; f)1300°C, mode III

stress due to the absence of interface delamination crack, resulting in high stress and strain concentration at the clad interface. However, under mode III, the main crack at the clad metal can propagate into the base metal as shown in Fig. 6f). Clad metal has higher fracture elongation and fracture toughness than the base metal and clad interface. The main crack can't be blunted and propagates into the base metal straightly, resulting in low bending toughness. Therefore, the fracture mode transmits from interfacial delamination into the crack branches with the increase of rolling temperature under modes II and III, respectively.

Fig. 7 shows the macroscopic impact fracture morphologies of stainless steel clad plates fabricated at different rolling temperature under mode I, and the values of experimental impact fracture energy are listed in Table 2. Obviously, all the stainless steel clad plates fabricated at 1100°C reveal interface delamination crack as shown in Figs. 7a), 7b) and 7c). Delamination crack enlarges the absorbed fracture energy because it makes the crack propagates long enough in comparison with the stainless steel clad plate with strong interface bonding [36]. Lesuer et al. [37] reported that if interface delamination occurs at the main crack tip, then the clad metal and base metal can deform individually under plane stress rather than plane strain condition. This change in deformation mode causes the individual layers to shear fracture fail and can increase the stress required for crack growing. That is to say, the impact toughness value tested on thick samples with multilayered structure and moderate interface is equal to the high toughness that would have been obtained for the individual thin layers under plane stress condition,

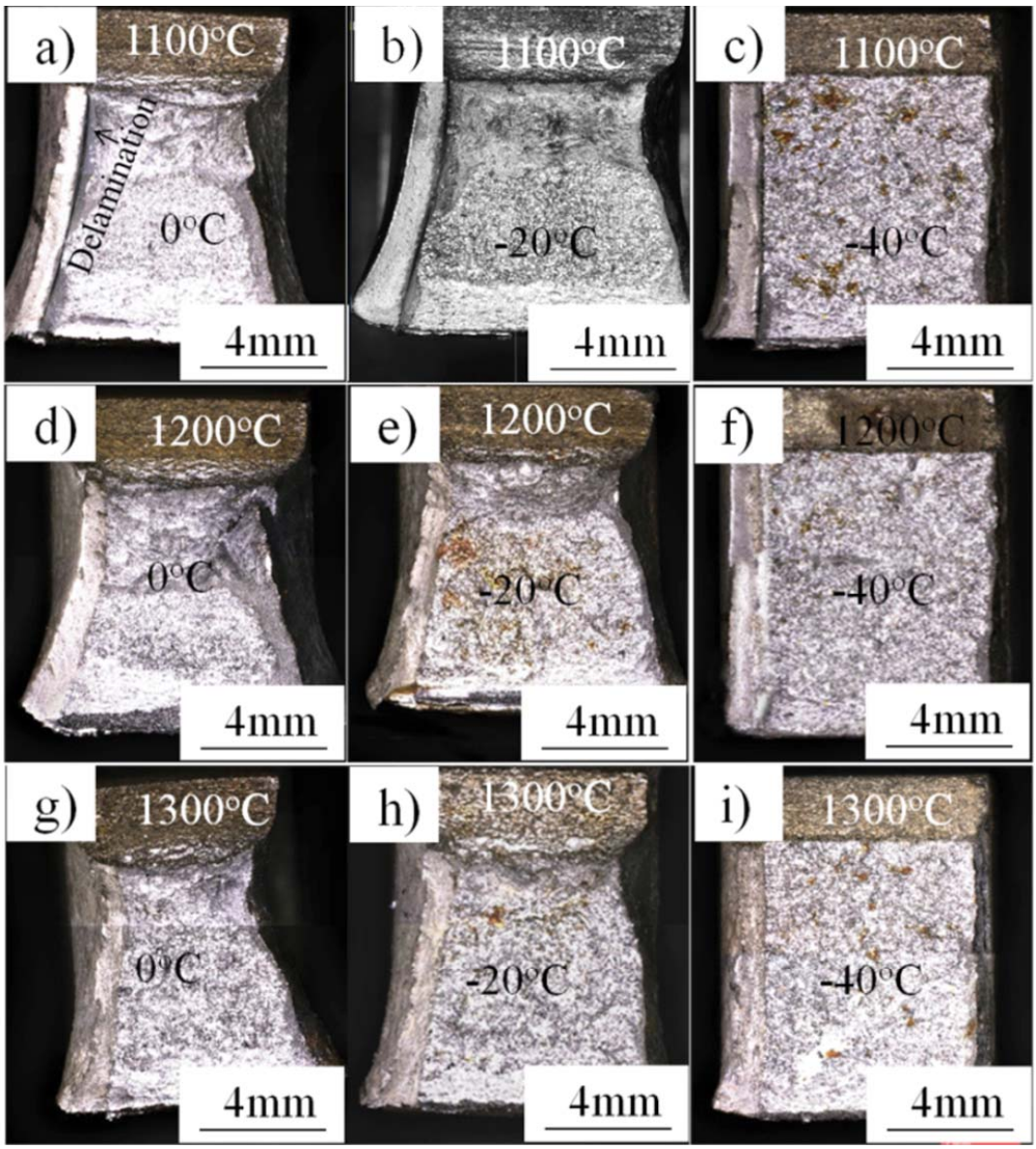

Fig. 7. The impact fracture morphologies of stainless steel clad plates with different rolling and testing temperatures under mode I. a) rolling temperature of 1100°C and testing temperature of 0°C; b) rolling temperature of 1100°C and testing temperature of –20°C; c) rolling temperature of 1100°C and testing temperature of –40°C; d) rolling temperature of 1200°C and testing temperature of 0°C; e) rolling temperature of 1200°C and testing temperature of –20°C; f) rolling temperature of 1200°C and testing temperature of –40°C; g) rolling temperature of 1300°C and testing temperature of 0°C; h)rolling temperature of 1300°C and testing temperature of –20°C; i) rolling temperature of 1300°C and testing temperature of –40°C

resulting in the local plane stress deformation and high impact toughness of stainless steel clad plates. Moreover, the refined microstructure and grain can also benefit to the enhanced impact toughness [11]. With the increase of rolling temperature, the impact toughness of stainless steel clad plate gradually decreasing as listed in Table 2. The impact fracture characteristics reveal gradually decreasing interface bonding strength of stainless steel clad plates. Especially at the rolling temperature of 1300°C, the absence of interface delamination and grains coarsening lead to the low impact toughness as shown in Figs. 7g)-i). In addition, with the decrease of testing temperature, the impact fracture characteristics change from axe-like shape to the brick-like shape, and the impact toughness decrease as listed in Table 2, which are fitting to the typical ductile-brittle transition of metal matrix composites.

Fig. 8 shows the impact fracture morphologies of stainless steel clad plates fabricated at different rolling temperature under

TABLE 2

The values of experimental impact fracture energy of stainless steel clad plates under modes I, II and III

Notch position (Profile cross-section) Mode I	**Rolling temperature**	**Experimental temperature**		
		0°C	**–20°C**	**–40°C**
	1100°C	116J	102J	20J
	1200°C	100J	80J	18J
	1300°C	75J	60J	15J
Notch position (carbon steel substrate) Mode II	**Rolling temperature**	**Experimental temperature**		
		0°C	**–20°C**	**–40°C**
	1100°C	48J	33J	12J
	1200°C	40J	30J	10J
	1300°C	16J	13J	10J
Notch position (stainless steel cladding) Mode III	**Rolling temperature**	**Experimental temperature**		
		0°C	**–20°C**	**–40°C**
	1100°C	162J	157J	150J
	1200°C	148J	150J	153J

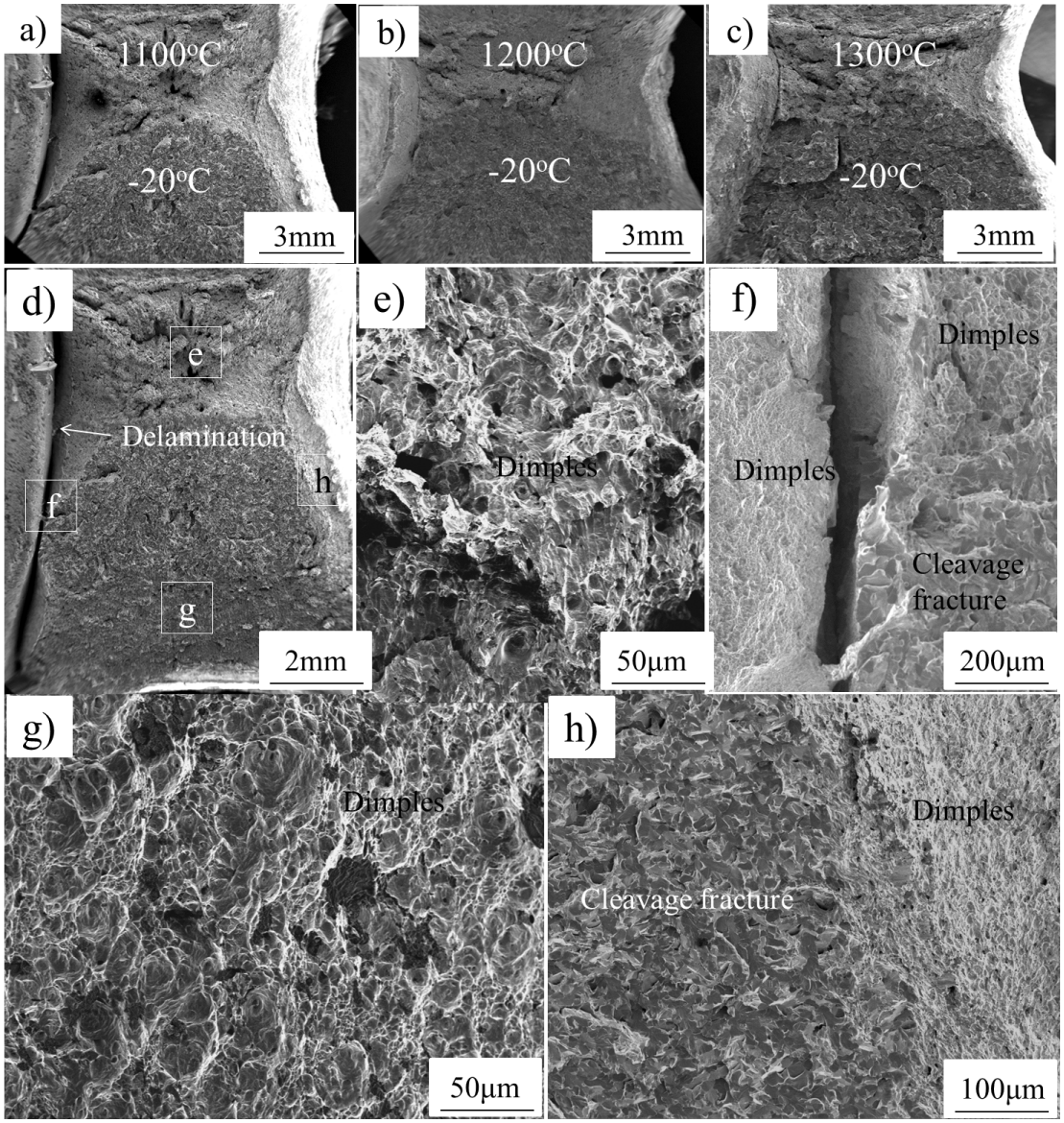

Fig. 8. The impact fracture morphologies of stainless steel clad plates with different rolling temperatures under I: a) 1100°C; b) 1200°C; c) 1300°C; the macroscopic impact fractrure characteristics of stainless steel clad plates fabricated at 1100°C under mode I: d) macro picture; e) fibrous zone; f) interface; g) compression stress zone; h) interface between radiation zone and shear lip

mode I. In addition to the interface delamination crack, the area of fibrous region displays a gradually decreased tread with the increasing rolling temperature as shown in Figs. 8a)-c), which reveals the ductile brittle transition phenomenon. Figs. 8d)-h) show the microscopic impact fracture characteristics of stainless steel clad plates fabricated at 1100°C under mode I. At the testing temperature of –20°C, an obvious interface delamination crack present at the clad interface as shown in Fig. 8d). One fourth of fracture area is comprised of fibrous zone, containing many dimples and revealing typical ductile fracture mode as shown in Fig. 8e). Interface delamination induces that individual layers deformed under plane strain conditions and enlarged the fibrous zone compared to the strong interface as shown in Fig. 8f). Individual layers experience considerable shear deformation and work hardening stages before fracture, resulting in super-high impact toughness. Fig. 8g) shows the typical ductile fracture characteristics away from the notch tip where the dimples appeared again. The reason is that compressive stress existed at the zones away from the notch tip. The crack is blocked when the crack encountered the compressive stress region. Fig. 8h) shows the interface fracture characteristics between radiation zone and shear lip. Obviously, the fracture mode of radiation zone is mainly dominated by cleavage fracture accompanying with many crack bifurcations, which is typical brittle fracture characteristics. However, the fracture mode varies from brittle fracture of radiation zone to ductile fracture of shear lip, which is attributed to the transition of stress state from plane strain to plane stress

Fig. 9 shows the impact fracture morphologies of stainless steel clad with different rolling and testing temperatures under mode II. Whatever the testing temperature is, the long interface delamination crack with extensive plastic deformation present at clad interface fabricated at 1100°C as shown in Figs. 9a)-c). Interface delamination enlarges the absorbed energy because that it inhibits the crack propagation in the stainless steel, which must deform plastically until a new dominant crack nucleate. Therefore, the main crack can't propagate into the clad metal. However, the stainless steel clad plates fabricated at 1200°C and 1300°C reveal a straight crack propagation path as shown in Fig. 9d)-i), and the main crack propagates into the stainless steel clad plate, resulting in low impact toughness.

Fig. 10 shows the impact fracture morphologies of stainless steel clad with different rolling and testing temperatures under mode II. At the rolling temperature of 1100°C, there are no any variations in the fracture morphology of clad plate under different testing temperature as shown in Figs. 10a)-c). A long interface delamination crack ahead of an advancing crack with the length of 1.5 mm present at the clad interface. Once the delamination crack occur, the stress concentration of main crack tip can be effectively relieved. These crack path deviations induce the main crack to move away from the plane experiencing maximum stress, and the stress state changes from triaxiality stress into the biaxial stress, displaying high impact energy. However, the stainless steel clad plate fabricated at 1200°C reveals slight interface delamination crack and severe crack bifurcation in the base metal as shown in Figs 10d)-f). Due to the strong interface, the main crack propagates into the base metal and leads to fracture failure of overall clad plate. Meanwhile, the crack bifurcation and local plastic deformation have occurred absence of stress relaxation at the interface. The crack bifurcation and plastic deformation consume a lot of fracture energy, resulting in similar super-high impact toughness with that of clad plate fabricated at 1100°C. In addition, the impact energy of mode III is the highest among the three modes, and testing temperature has few influences on

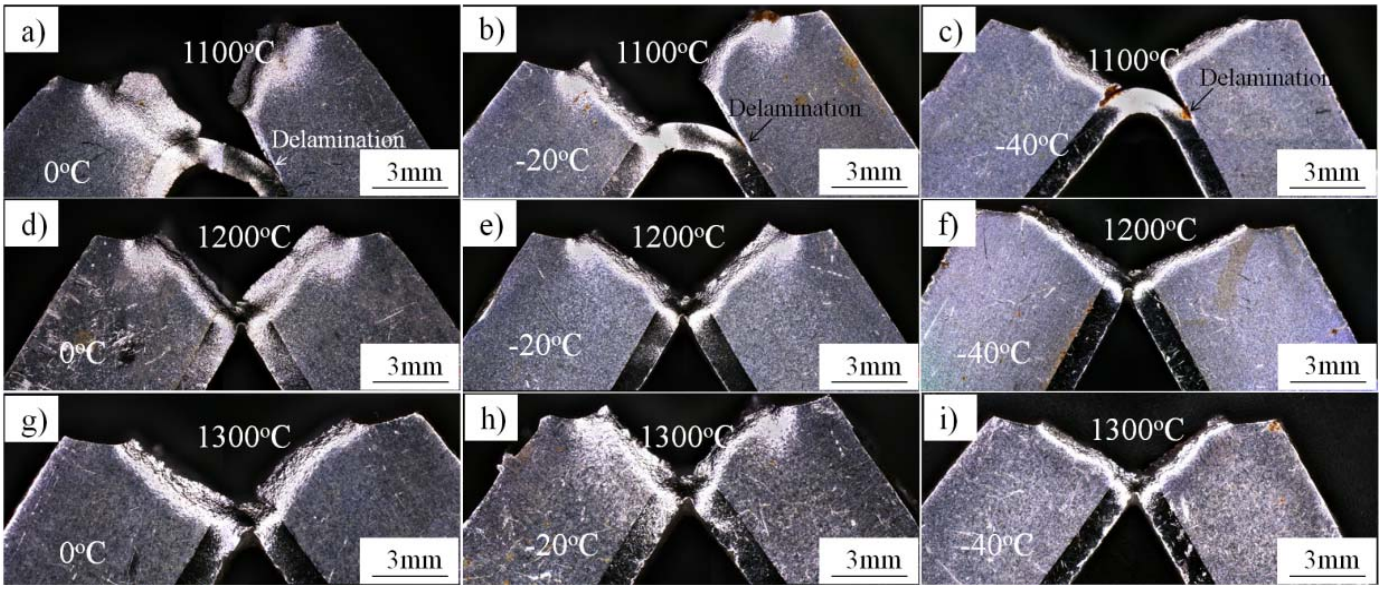

Fig. 9. The impact fracture morphologies of stainless steel clad with different rolling and testing temperatures under mode II. a) rolling temperature of 1100°C and testing temperature of 0°C; b) rolling temperature of 1100°C and testing temperature of –20°C; c) rolling temperature of 1100°C and testing temperature of –40°C; d) rolling temperature of 1200°C and testing temperature of 0°C; e) rolling temperature of 1200°C and testing temperature of –20°C; f) rolling temperature of 1200°C and testing temperature of –40°C; g) rolling temperature of 1300°C and testing temperature of 0°C; h)rolling temperature of 1300°C and testing temperature of –20°C; i) rolling temperature of 1300°C and testing temperature of –40°C

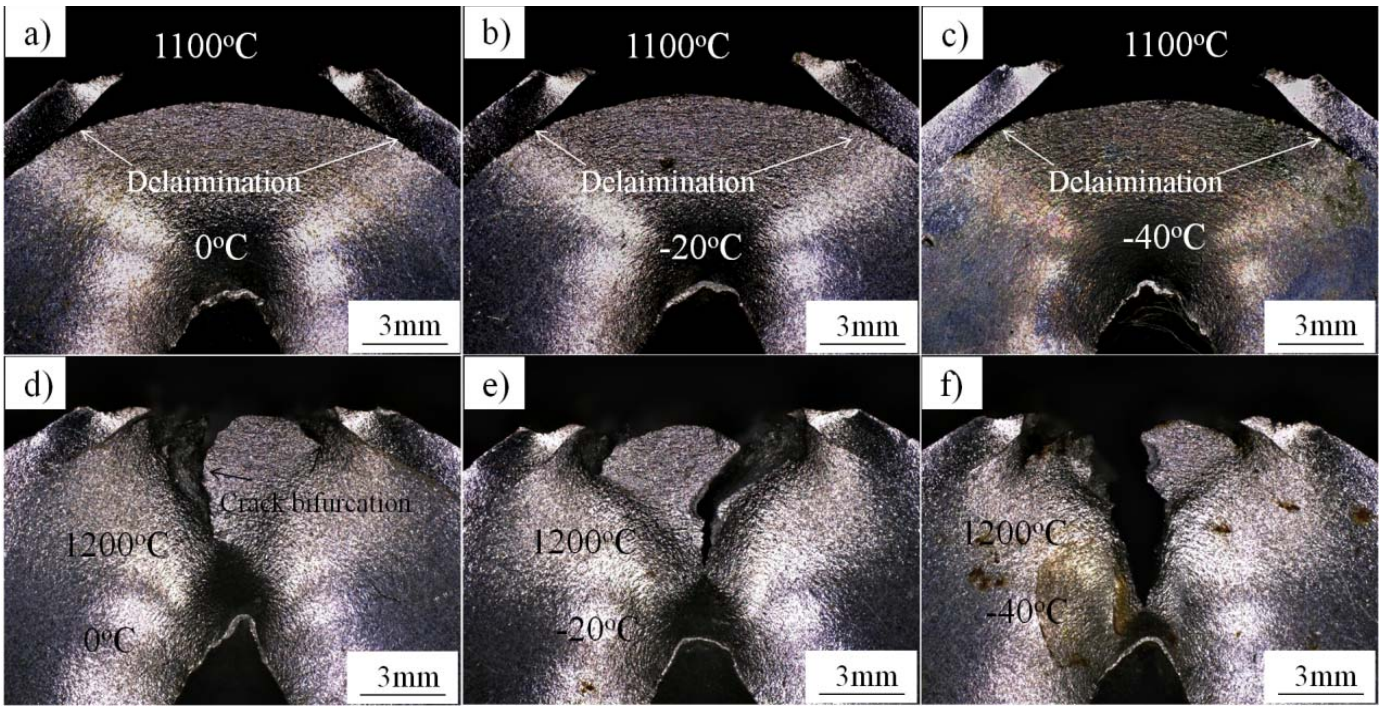

Fig. 10. The impact fracture morphologies of stainless steel clad with different rolling and testing temperatures under mode III. a) rolling temperature of 1100°C and testing temperature of 0°C; b) rolling temperature of 1100°C and testing temperature of –20°C; c) rolling temperature of 1100°C and testing temperature of –40°C; d) rolling temperature of 1200°C and testing temperature of 0°C; e) rolling temperature of 1200°C and testing temperature of –20°C; f) rolling temperature of 1200°C and testing temperature of –40°C

the impact energy under mode III. The high impact energy of mode III is attributed to that crack initiation zone present at the clad metal, as well as the nonstandard notch with small size. Also in mode II, low impact energy has obtained that crack propagated through carbon steel.

4. Conclusions

(1) The interface bonding strength gradually increase, whereas bending strength decrease with the increase of rolling temperature, which is attributed to matrix softening effect and alloy element diffusion behavior.
(2) The average length of interface delamination cracks gradually decrease with the increase of rolling temperature, leading to the gradually decrease of impact toughness under modes I and II.
(3) Stainless steel clad plates fabricated at 1100°C and 1200°C obtain similar impact energy under mode III. Long delamination toughening mechanism is located at the clad plate fabricated at 1100°C, whereas the clad plate fabricated at 1200°C contains delamination crack and crack bifurcation competing mechanisms.

Acknowledgements

This work is financially supported by the National Natural Science Foundation of China (NSFC) under Grant No. 51601055, the Natural Science Foundation of Hebei Province under Grant No. E2018202245, the Joint Fund for Steel Research of National Natural Science Foundation of China and Baowu Steel Group Corporation Limited (No. U1860114), the Technology Innovation Strategy Funding Project of Hebei Science and Technology Department and Hebei University of Technology (No. 20180106), the "One Belt and One Road" Technology Innovation Cooperation Project of Tianjin (No. 18PTZWHZ00220), the Key Research and Development Program of Hebei Province, China (No. 17391001D).

REFERENCES

[1] Z. Dhib, N. Guermazi, A. Ktari, M. Gasperini, N. Haddar, Mechanical bonding properties and interfacial morphologies of austenitic stainless steel clad plates. Materials Science and Engineering A **696**, 374-386 (2017).
[2] H. Song, H. Shin, Y. Shin, Heat treatment of clad steel plate for application of hull structure. Ocean Engineering **122**, 278-287 (2016).
[3] Z.C. Zhu, Y. He, X.J. Zhang, H.Y. Liu, X. Li, Effect of interface oxides on shear properties of hot-rolled stainless steel clad plate. Materials Science and Engineering A **669**, 344-349 (2016).
[4] B. Aleman, I. Gutierrez, J.J. Urcola, Interface microstructures in diffusion bonding of titanium alloys to stainless and low alloy steel. Materials Science and Technology **9**, 633-641 (1993).
[5] J. Pavlovsky, B. Million, K. Ciha, K. Stransky, Carbon redistribution between an austenitic cladding and a ferritic steel for pressure vessels of nuclear reactor. Materials Science and Engineering A **149**, 105-110 (1991).

[6] L. Li, F.X. Yin, K. Nagai, Progress of laminated materials and clad steels production. Materials Science Forum **675-677**, 439-447 (2011).

[7] G.M. Xie, Z.G. Luo, G.L. Wang, L. Li, G.D. Wang, Interface characteristic and properties of stainless steel/HSLA steel clad plate by vacuum rolling cladding. Materials Transactions **52**, 1709-1712 (2011).

[8] A.K. Motarjemi, M. Kocak, V. Ventzke, Mechanical and fracture characterization of a bi-material steel plate. International Journal of Pressure Vessels and Piping **79**, 181-191 (2002).

[9] Z. Dhib, N. Guermazi, M. Gasperini, N. Haddar, Cladding of low-carbon steel to austenitic stainless steel by hot-roll bonding: microstructure and mechanical properties before and after welding. Materials Science and Engineering A **656,** 130-141 (2016).

[10] C.X. Chen, M.Y. Liu, B.X. Liu, F.X. Yin, Y.C. Dong, X. Zhang, F.Y. Zhang, Y.G. Zhang, Tensile shear sample design and interfacial shear strength of stainless steel clad plate. Fusion Engineering and Design. 2017. In Press.

[11] B.X. Liu, F.X. Yin, X.L. Dai, J.N. He, W. Fang, C.X. Chen, Y.C. Dong, The tensile behaviors and fracture characteristics of stainless steel clad plates with different interfacial status. Materials Science and Engineering A **679**, 172-182 (2017).

[12] B.X. Liu, L.J. Huang, B. Kaveendran, L. Geng, X.P. Cui, S.L. Wei, F.X. Yin, Tensile and bending behaviors and characteristics of laminated Ti-(TiBw/Ti) composites with different interface status. Composites Part B **108**, 377-385 (2017).

[13] D.W. Kum, T. Oyama, J. Wadsworth, O.D. Sherby, The impact properties of laminated composites containing ultrahigh carbon (UHC) steels. J. Mech. Phys. Solids **31**, 173-186 (1983).

[14] M. Koyama, Z. Zhang, M.M. Wang, D. Ponge, D. Raabe, K. Tsuzaki, H. Noguchi, C.C. Tasan, Bone-like crack resistance in hierarchical metastable nanolaminate steel. Science **355**, 1055-1057 (2017).

[15] B.X. Liu, L.J. Huang, X.D. Rong, L. Geng, F.X. Yin, Bending behaviors and fracture characteristics of laminated ductile-tough composites under different modes. Composites Science and Technology **126**, 94-105 (2016).

[16] Y. Ohashi, J. Wolfenstine, R. Koch, O.D. Sherby, Fracture behavior of a laminated steel-brass composite in bend tests. Materials Science and Engineering A **151**, 37-44 (1992).

[17] O.D. Sherby, S. Lee, R. Koch, T. Sumi, J. Wolfenstine, Multilayered composites based on ultrahigh carbon steel and brass. Materials and Manufacturing Processes **5**, 363-376 (1990).

[18] Y. Kimura, T. Inoue, F.X. Yin, K. Tsuzaki, Inverse temperature dependence of toughness in an ultrafine grain-structure steel. Science **320**, 1057-1060 (2008).

[19] J. Cook, J.E. Gordon, C.C. Evans, D.M. Marsh, A Mechanisms for the control of crack propagation in all-brittle systems. Proceedings of Royal Society of London **282**, 508-520 (1964).

[20] S. Lee, T. Oyama, J. Wolfenstine, O.D. Sherby, Impact properties of a laminated composite based on ultrahigh carbon steel and brass. Materials Science and Engineering A 154, **133-137** (1992).

[21] F. Song, Y.L. Bai, Effects of nanostructures on the fracture strength of the interfaces in nacre. J. Mater. Res. **18**, 1741-1744 (2003).

[22] Y. Jing, Y. Qin, X.M. Zang, Q.Y. Shang, H. Song, A novel reduction-bonding process to fabricate stainless steel clad plate. Journal of Alloys and Compounds **617**, 688-698 (2014).

[23] Y. Jing, Y. Qin, X.M. Zang, Y.H. Li, The bonding properties and interfacial morphologies of clad plate prepared by multiple passes hot rolling in a protective atmosphere. Journal of Materials Processing Technology **214** ,1686-1695 (2014).

[24] Z.J. Wu, W.F. Peng, X.D. Shu, Influence of rolling temperature on interface properties of the cross wedge rolling of 42CrMo/Q235 laminated shaft. Int. J. Adv. Manuf. Technol. **91**, 517-526 (2017).

[25] O. Hedayati, N. Korei, M. Adeli, M. Etminanbakhsh, Microstructural evolution and interfacial diffusion during heat treatment of Hastelloy/stainless steel bimetals. Journal of Alloys and Compounds **712**, 172-178 (2017).

[26] B.X. Liu, L.J. Huang, L. Geng, B. Kaveendran, B. Wang, X.Q. Song, X.P. Cui, Gradient grain distribution and enhanced properties of novel laminated Ti-TiBw/Ti composites by reaction hot pressing. Materials Science & Engineering A **595**, 257-265 (2014).

[27] L. Kolarik, J. Janovec, M. Kolarikova, P. Nachtnebl, Influence of diffusion welding time on homogenous steel joints. Procedia Engineering **100**, 1678-1685 (2015).

[28] G.L. Wang, Research on interface inclusions' evolution mechanism and process control of vacuum hot roll-cladding. Doctor thesis of northeastern university. 2013. 1-162 (in Chinese).

[29] X.N. Guo, Y. He. X.J. Zhang, M.N. Li, Microstructure and mechanical properties of binding interface between hot-rolled stainless steel/carbon steel clad plates. Cfhi Technology **52-55**,167 (2015) (in Chinese).

[30] R. Ayer, R.R. Mueller, D.P. Leta, W.J. Sisak, Phase transformations at steel/in625 clad interfaces. Metallurgical Transactions A **20**, 665-681 (1989).

[31] F. Mas, C. Tassin, N. Valle, F. Robaut, F. Charlot, M. Yescas, F. Roch, P. Todeschini, Y. Brechet, Metallurgical characterization of coupled carbon diffusion and precipitation in dissimilar steel welds. Journal of Materials Science **51**, 4846-4879 (2016).

[32] H.X. Mei, Y.Y. Pang, R. Huang, Influence of interfacial delamination on channel cracking of elastic thin films. International Journal of Fracture **148**, 331-342 (2007).

[33] J.L. Beuth, S.H. Narayan, Residual stress-driven delamination in deposited multilayers. Int. J. Solids Structures **33**, 65-78 (1996).

[34] B.S. Li, J.L. Shang, J.J. Guo, H.Z. Fu, In situ observation of fracture behavior of in situ TiBw/Ti composites. Materials Science and Engineering A **383**, 316-322 (2004).

[35] B.X. Liu, L. Geng, X.L. Dai, F.X. Yin, L.J. Huang, Multiple toughening mechanisms of laminated Ti-TiBw/Ti composites fabricated by diffusion welding **84**, 196-201 (2016).

[36] C.M. Cepeda-Jimenez, F. Carreno, O.A. Ruano, A.A. Sarkeeva, A.A. Kruglov, R.Ya. Lutfullin, Influence of interfacial defects on the impact toughness of solid state diffusion bonded Ti-6Al-4V alloy based multilayer composites. Materials Science and Engineering A **563**, 28-35 (2013).

[37] D.R. Lesuer, C.K. Syn, O.D. Sherby, J. Wadsworth, J.J. Lewandowski, W.H. Hunt, Mechanical behavior of laminated metal composites. International Materials Reviews **41**, 169-197 (1996).